ATLAS NOTE

ATLAS-CONF-2012-170

December 14 2012
Minor revision: January 3 2013

An update of combined measurements of the new Higgs-like boson with high mass resolution channels

The ATLAS Collaboration

Abstract

An update is presented of the measurement of the newly discovered boson properties using the high mass resolution channels, $H\to\gamma\gamma$ and $H\to ZZ^{(*)}\to 4\ell$, with up to 4.8 fb^{-1} of pp collision data at $\sqrt{s}$ = 7 TeV and 13 fb^{-1} at $\sqrt{s}$ = 8 TeV. The combined mass measurement derived from the $H\to\gamma\gamma$ and $H\to ZZ^{(*)}\to 4\ell$ channels is $m_H = 125.2 \pm 0.3\,(\text{stat}) \pm 0.6\,(\text{sys})$ GeV. The combination of all final states, including the recently updated low mass resolution channels $H\to WW^{(*)}\to \ell\nu\ell\nu$, $H\to\tau^+\tau^-$ and $H\to b\bar{b}$, is reported for this data set in terms of the combined signal strength (μ). This is determined to be $\mu = 1.35 \pm 0.24$ computed at a mass of 125 GeV, in agreement with the Standard Model expectation.

Revised based on the version released on 14th, December 2012 (textual correction of the number of categories in the $H\to\gamma\gamma$ channel for the 2011 data analysis).

1 Introduction

The observation of a new particle in the search for the Standard Model (SM) Higgs boson at the LHC, reported by the ATLAS [1] and CMS [2] Collaborations, is a milestone in the quest to understand electroweak symmetry breaking. In Refs. [1] and [3] the ATLAS Collaboration reported estimates for the mass of the particle and its coupling properties. An update of the combined signal strength value for low mass resolution channels $H \to WW^{(*)} \to \ell\nu\ell\nu$, $H \to \tau^+\tau^-$ and $H \to b\bar{b}$ has been reported in Ref. [4]. This document presents an update of the measurements of the mass and signal strength of the observed new particle using up to 4.8 fb^{-1} of pp collision data at $\sqrt{s}$ = 7 TeV and 13 fb^{-1} at $\sqrt{s}$ = 8 TeV for the five main channels, including the $H \to \gamma\gamma$ [5] and $H \to ZZ^{(*)} \to 4\ell$ [6] channels.

The results are based on the same statistical model as in Refs. [1, 3] describing the experimental and theoretical systematic uncertainties. The aspects of the individual channels relevant for these measurements are briefly summarized in Section 2. The statistical procedure is outlined in Section 3. As the $H \to \gamma\gamma$ and $H \to ZZ^{(*)} \to 4\ell$ mass measurements show a sizeable difference, the systematic uncertainties that contribute to these measurements are discussed in detail in Section 4. The measurement of the mass, obtained from the $H \to \gamma\gamma$ and $H \to ZZ^{(*)} \to 4\ell$ channels, is described in Section 5. Finally, measurements of the signal strength μ and the significance are presented in Section 6.

2 Individual Channels

For the $H \to \tau^+\tau^-$ and $H \to b\bar{b}$ channels, the updated analyses [7, 8] are applied to the full available 2011 data sample at $\sqrt{s}$ = 7 TeV and the available 2012 data sample at $\sqrt{s}$ = 8 TeV . For the $H \to WW^{(*)} \to \ell\nu\ell\nu$ final state, only the latest ATLAS results [9], based on the different flavour ($e\mu$ and μe) 0-jet and 1-jet analyses in the 2012 data, are considered here. For the $H \to \gamma\gamma$ and $H \to ZZ^{(*)}$ channels, the updated analyses as presented in Refs. [5,6] are used. The different final states and channel categories considered in this analysis are summarized in Table 1.

3 Likelihood Parametrization and Statistical Procedure

The statistical modelling of the data is described in Refs. [10–14]. Given the observed data, the resulting likelihood function is parametrized in terms of scale factors for the cross-section of each SM Higgs production mode, the branching ratios of the SM Higgs boson decays, and the mass of the Higgs boson m_H. In addition, the global signal strength factor, μ, acts as a scale factor on the total number of events predicted by the Standard Model for the Higgs boson signal. This scale factor is defined such that $\mu = 0$ corresponds to the background-only hypothesis and $\mu = 1$ corresponds to the SM Higgs boson signal in addition to the background. In order to assess the mass measurement compatibility, the measured mass of the particle is distinguished in the high-resolution $H \to ZZ^{(*)} \to 4\ell$ and $H \to \gamma\gamma$ channels, denoted $m_H^{4\ell}$ and $m_H^{\gamma\gamma}$ with $\Delta m_H \equiv m_H^{\gamma\gamma} - m_H^{4\ell}$. Finally, the full set of nuisance parameters associated with the systematic uncertainties is denoted $\boldsymbol{\theta}$.

Hypothesis testing and confidence intervals are based on the profile likelihood ratio [15]. The parameters of interest depend on the test in question, while the remaining parameters are profiled. As indicated in the sections below, the mass parameter m_H may either be fixed, an explicit parameter of interest, or profiled.

The treatment of systematic uncertainties and their correlations is described in detail in Ref. [16]. Systematic uncertainties on observables are handled by introducing nuisance parameters with a probability density function (pdf) associated with the estimate of the corresponding effect. These nuisance parameters, in particular those representing instrumental uncertainties or background estimates, are often assessed from auxiliary measurements, such as control regions, sidebands, or dedicated calibration measurements. Their pdf is described either by a Gaussian or alternatively by a log-normal distribution to avoid the truncation of a pdf bounded to a restricted range, which should be an accurate description for most cases. In cases where the uncertainty is related to a number of events (*e.g.* from Monte Carlo or data control samples) the Poisson function is used.

4 Systematic Uncertainties on Mass Measurements

The systematic uncertainties considered in the individual channels form the basis of the combined models. A complete description of these individual systematic uncertainties is given in Refs. [5–9]. The model of the correlations between channels and between signal and background is taken into account and follows essentially the scheme described in Refs. [1, 10]. In this section, only the main uncertainties pertaining to the combined measurement of the mass are discussed.

Systematic uncertainties on the mass measurement in the $H \to \gamma\gamma$ channel arise mainly from the uncertainties on the photon energy scale. The electromagnetic calorimeter energy scale is set using the high statistics sample of electrons from $Z \to ee$ decays (about 5M events for the full sample analysed to date in 2011 and 2012). A comprehensive set of detector-related uncertainties on the mass measurement,

Table 1: Summary of the individual channels entering the combined results presented here. In channels sensitive to associated production of the Higgs boson, V indicates a W or Z boson. The symbols $\otimes$ and $\oplus$ represent direct products and sums over sets of selection requirements, respectively. The abbreviations listed here are described in the corresponding Refs. reported in the last column.

Higgs Boson Decay	Subsequent Decay	Sub-Channels	$\int L\,dt$ [fb^{-1}]	Ref.
		2011 $\sqrt{s}$ =7 TeV		
$H \to ZZ^{(*)}$	4ℓ	$\{4e, 2e2\mu, 2\mu 2e, 4\mu\}$	4.6	[1]
$H \to \gamma\gamma$	–	10 categories $\{p_{\mathrm{Tt}} \otimes \eta_\gamma \otimes$ conversion$\} \oplus \{$2-jet VBF$\} \oplus \{\ell$-tag, 2-jet VH$\}$	4.8	[5]
$H \to \tau\tau$	$\tau_{\mathrm{lep}}\tau_{\mathrm{lep}}$	$\{e\mu\} \otimes \{$0-jet$\} \oplus \{\ell\ell\} \otimes \{$1-jet, 2-jet, $p_{\mathrm{T},\tau\tau} > 100$ GeV, $VH\}$	4.6	[7]
	$\tau_{\mathrm{lep}}\tau_{\mathrm{had}}$	$\{e, \mu\} \otimes \{$0-jet, 1-jet, $p_{\mathrm{T},\tau\tau} > 100$ GeV, 2-jet$\}$	4.6	
	$\tau_{\mathrm{had}}\tau_{\mathrm{had}}$	$\{$1-jet, 2-jet$\}$	4.6	
$VH \to Vbb$	$Z \to \nu\nu$	$E_{\mathrm{T}}^{\mathrm{miss}} \in \{120-160, 160-200, \geq 200$ GeV$\} \otimes \{$2-jet, 3-jet$\}$	4.6	[8]
	$W \to \ell\nu$	$p_{\mathrm{T}}^{W} \in \{< 50, 50-100, 100-150, 150-200, \geq 200$ GeV$\}$	4.7	
	$Z \to \ell\ell$	$p_{\mathrm{T}}^{Z} \in \{< 50, 50-100, 100-150, 150-200, \geq 200$ GeV$\}$	4.7	
		2012 $\sqrt{s}$ =8 TeV		
$H \to ZZ^{(*)}$	4ℓ	$\{4e, 2e2\mu, 2\mu 2e, 4\mu\}$	13	[6]
$H \to \gamma\gamma$	–	12 categories $\{p_{\mathrm{Tt}} \otimes \eta_\gamma \otimes$ conversion$\} \oplus \{$2-jet VBF$\} \oplus \{\ell$-tag, 2-jet VH$\}$	13	[5]
$H \to WW^{(*)}$	$e\nu\mu\nu$	$\{e\mu, \mu e\} \otimes \{$0-jet, 1-jet$\}$	13	[9]
$H \to \tau\tau$	$\tau_{\mathrm{lep}}\tau_{\mathrm{lep}}$	$\{\ell\ell\} \otimes \{$1-jet, 2-jet, $p_{\mathrm{T},\tau\tau} > 100$ GeV, $VH\}$	13	[7]
	$\tau_{\mathrm{lep}}\tau_{\mathrm{had}}$	$\{e, \mu\} \otimes \{$0-jet, 1-jet, $p_{\mathrm{T},\tau\tau} > 100$ GeV, 2-jet$\}$	13	
	$\tau_{\mathrm{had}}\tau_{\mathrm{had}}$	$\{$1-jet, 2-jet$\}$	13	
$VH \to Vbb$	$Z \to \nu\nu$	$E_{\mathrm{T}}^{\mathrm{miss}} \in \{120-160, 160-200, \geq 200$ GeV$\} \otimes \{$2-jet, 3-jet$\}$	13	[8]
	$W \to \ell\nu$	$p_{\mathrm{T}}^{W} \in \{< 50, 50-100, 100-150, 150-200, \geq 200$ GeV$\}$	13	
	$Z \to \ell\ell$	$p_{\mathrm{T}}^{Z} \in \{< 50, 50-100, 100-150, 150-200, \geq 200$ GeV$\}$	13	

arising from a number of sources and estimated as relative contributions to the total uncertainty on the measured Higgs-boson mass, are listed below and detailed in Ref. [5]:

- The uncertainty on the absolute energy scale calibration factors derived from $Z \rightarrow ee$ events is estimated to be $\pm$ 0.3%.
- The uncertainty due to the imperfect knowledge of the material upstream of the electromagnetic calorimeter is estimated to be $\pm$ 0.3%. This systematic uncertainty is estimated using samples simulated with relative changes to the upstream material description of 5-10%. Such a variation is larger than that indicated by the level of agreement between data and simulation, in studies of the track reconstruction efficiency for charged pions, of low-energy converted photon rates, and of the modelling of the longitudinal shower shapes in the electromagnetic calorimeter.
- The relative calibration of the different layers of the electromagnetic calorimeter, namely $\pm$ 0.1% from the presampler energy scale and $\pm$0.2% from the relative calibration of the strip layer compared to the middle layer.
- The uncertainty related to differences in lateral shower development between electrons and photons is estimated to be $\pm$ 0.1% as measured with radiative Z boson events.
- The uncertainty related to the different mix of readout electronics gain between electrons in $Z \rightarrow ee$ and photons in $H \rightarrow \gamma\gamma$ is estimated to be $\pm$ 0.15%.
- The impact of pile-up, estimated to be well below $\pm$ 0.1%, is neglected.

Other analysis-related uncertainties on the mass measurement were also investigated:

- possible differences between data and simulation in the classification of photon candidates in the converted category, originating from the wrong association of a photon cluster with an unrelated track, estimated to be $\pm$ 0.13%;
- variations arising from the use of alternative background models in the extraction of the mass of the observed signal, estimated to be $\pm$ 0.1%;
- the stability of the mass measurement under variations of the mass resolution, resulting in an overall uncertainty of $\pm$ 0.15%;
- possible systematic biases on the measurements of the photon angles, estimated to be $\pm$ 0.03%, as obtained from studies reconstructing data $Z \rightarrow ee$ decays using only the electromagnetic calorimeter information for the electron angles.

The total systematic uncertainty on the mass measurement in the $H \rightarrow \gamma\gamma$ channel amounts to $\pm$0.7 GeV, while the statistical uncertainty is $\pm$0.3 GeV. Several additional cross-checks have been performed on the stability and robustness of this result and none of them indicates any systematic effect not covered by the uncertainties described above. An independent cross-check is obtained by determining the photon energy scale directly, using a dataset of radiative $Z \rightarrow \ell\ell$ decays, albeit over a lower energy range not overlapping fully with that from $H \rightarrow \gamma\gamma$ decays. The measured value of the Z-boson mass in these events is consistent with the expectation.

The systematic uncertainty on the mass measurement in the $H \rightarrow ZZ^{(*)} \rightarrow 4\ell$ channel is discussed in Ref. [6] and is dominated by contributions related to the muon momentum measurement, since the $H \rightarrow 4\mu$ channel is the one with the largest event yield, the best mass resolution and the lowest background. The various components of the detector-related systematic uncertainty are determined using large samples of $J/\psi \to \mu\mu$, $\Upsilon \to \mu\mu$ and $Z \to \mu\mu$ decays (more than 20M J/ψ decays have been collected in both 2011 and 2012). These large samples allow precise determinations of possible global mass scale biases found to be below 0.1% in both the inner detector and the muon spectrometer which provide independent measurements of the muon momentum. They also provide the possibility of probing local charge-symmetric scale biases and global and local charge-asymmetric scale biases, all of which affect only the mass resolution, for samples with high statistics. The overall uncertainty on the muon momentum scale is estimated to be ± 0.2% for the $H \to 4\mu$ channel. In addition, the local biases mentioned above are assessed for each muon from the low-statistics sample of $H \to 4\mu$ candidate events and their impact on the mass measurement and its error is found to be negligible, i.e. below 0.1 GeV.

For the $H \to ZZ^{(*)} \to 4\ell$ decay modes involving electrons, the impact of the electron energy scale uncertainty is estimated in a similar manner as for photons. However, the only sizeable systematic uncertainty fully correlated with photons is the uncertainty on the electron energy scale extraction from the $Z \to ee$ sample. For electrons the impact of the energy scale uncertainty on the $H \to eeee$ final state is estimated to be ± 0.4%. The uncertainty on the energy scale for electrons with transverse energies below 15 GeV is obtained using $J/\psi \to e^+e^-$ decays: for electrons with a transverse energy of ~ 10 GeV, the measurements agree with the predictions to better than 1%, which leads to a negligible contribution to the overall uncertainty in the $H \to ZZ^{(*)} \to 4\ell$ mass measurement, i.e. below ± 0.1%. Finally, mass scale uncertainties related to final-state QED radiation modelling and to background contamination are also smaller than ± 0.1%.

The total systematic uncertainty on the mass measurement in the $H \to ZZ^{(*)} \to 4\ell$ channel thus amounts to ±0.3 GeV, while the statistical uncertainty is ±0.9 GeV, as evaluated from pseudo-experiments.

Most of the uncertainties mentioned above are of the type where an *a priori* pdf is not defined. For practical purposes a Gaussian constraint is used for these uncertainties. However, an alternative choice of pdf is a rectangular distribution[1], as discussed in Ref. [3] and subsection 5.2.

5 Mass measurement

The mass of the newly discovered boson can be measured precisely in the high mass resolution channels $H \to \gamma\gamma$ and $H \to ZZ^{(*)} \to 4\ell$. A mass of $m_H = 126.6 \pm 0.3\,(\text{stat}) \pm 0.7\,(\text{sys})$ GeV is found in the $H \to \gamma\gamma$ channel [5] and a mass of $m_H = 123.5 \pm 0.8\,(\text{stat}) \pm 0.3\,(\text{sys})$ GeV in the $H \to ZZ^{(*)} \to 4\ell$ channel [6], with systematic errors which are largely uncorrelated, as discussed below. In Ref. [6] the quoted result uses Monte Carlo pseudo-experiments to estimate the statistical uncertainty. This gives a slightly larger statistical error, corresponding to ±0.9 GeV, compared to the one obtained with the asymptotic approximation leaving the mean value and the systematic uncertainty unchanged. Since the combination below relies on the asymptotic method, the corresponding $H \to ZZ^{(*)} \to 4\ell$ uncertainty from the asymptotic approximation is quoted here.

5.1 Combined mass estimates from the $H \to \gamma\gamma$ and $H \to ZZ^{(*)} \to 4\ell$ channels

An estimate of the mass of the Higgs-boson like particle, combining the $H \to \gamma\gamma$ and $H \to ZZ^{(*)} \to 4\ell$ channels, is based on the profile likelihood ratio

$$\Lambda(m_H) = \frac{L(m_H\,,\, \hat{\hat{\mu}}_{\gamma\gamma}(m_H)\,,\, \hat{\hat{\mu}}_{4\ell}(m_H)\,,\, \hat{\hat{\boldsymbol{\theta}}}(m_H))}{L(\hat{m}_H, \hat{\mu}_{\gamma\gamma}, \hat{\mu}_{4\ell}, \hat{\boldsymbol{\theta}})}\ . \tag{1}$$

where the single circumflex denotes the unconditional maximum likelihood estimate of a parameter and the double circumflex (*e.g.* $\hat{\hat{\boldsymbol{\theta}}}(m_H)$) denotes the conditional maximum likelihood estimate (*e.g.* of $\boldsymbol{\theta}$)

[1]Nuisance parameters are treated as unconstrained with a flat pdf in the interval defined by ±1 units of their estimated uncertainty.

for given fixed values of m_H. This estimate allows the signal strength to vary independently in the two channels (treating both signal strengths as nuisance parameters), while the ratios of the cross-sections in the different production modes within each channel are fixed to the SM. The leading source of systematic uncertainty in the mass estimate comes from the mass scale systematic uncertainties which are described in detail in Section 4. Figure 1 shows the profile likelihood ratio as a function of m_H for the $H\rightarrow\gamma\gamma$ and $H\rightarrow ZZ^{(*)}\rightarrow 4\ell$ channels and the combination. From the $H\rightarrow\gamma\gamma$ and $H\rightarrow ZZ^{(*)}\rightarrow 4\ell$ combination the common mass is estimated to be

$$m_H = 125.2 \pm 0.7 \text{ GeV} = 125.2 \pm 0.3\,(\text{stat}) \pm 0.6\,(\text{sys}) \text{ GeV} . \quad (2)$$

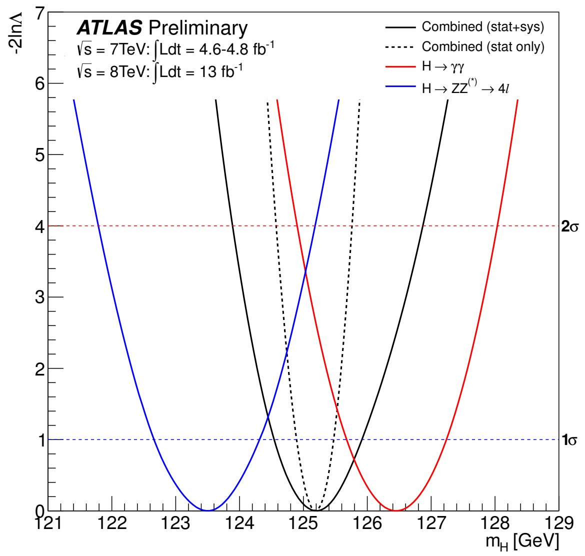

Figure 1: The profile likelihood ratio $-2\ln\Lambda(m_H)$ as a function of m_H for the $H\rightarrow\gamma\gamma$ and $H\rightarrow ZZ^{(*)}\rightarrow 4\ell$ channels and the combination, allowing the signal strengths $\mu_{\gamma\gamma}$ and $\mu_{4\ell}$ to vary independently. The dashed line shows the statistical component of the mass measurement.

5.2 Consistency of mass estimates from $H\rightarrow\gamma\gamma$ and $H\rightarrow ZZ^{(*)}\rightarrow 4\ell$

To assess the consistency of the two mass measurements we first consider a likelihood function in which the mass parameters $m_H^{\gamma\gamma}$ and $m_H^{4\ell}$ vary independently. Figure 2(a) shows likelihood contours in $m_H^{\gamma\gamma}$ and $m_H^{4\ell}$ around the two independent best fit mass values and the best fit point for $\hat{m}_H = \hat{m}_H^{\gamma\gamma} = \hat{m}_H^{4\ell}$. As this plot shows, the two mass measurements are almost uncorrelated. The largest correlation between the measurements is the overall e/γ energy scale from the $Z \rightarrow e^+e^-$ calibration, which affects mostly the $H\rightarrow\gamma\gamma$ channel, as the $H\rightarrow ZZ^{(*)}\rightarrow 4\ell$ channel is dominated by 4μ-events. However, the mass consistency between muon and electron final states in the $H\rightarrow ZZ^{(*)}\rightarrow 4\ell$ channel causes a $\sim 0.3\sigma$ adjustment in the overall e/γ energy scale which induces an approximate 0.1% downward shift in $m_H^{\gamma\gamma}$ in the combination.

To directly quantify the level of consistency between the measurements of $m_H^{\gamma\gamma}$ and $m_H^{4\ell}$, a likelihood function is considered for the mass difference $\Delta m_H = m_H^{\gamma\gamma} - m_H^{4\ell}$, with the common mass m_H profiled in the fit:

$$\Lambda(\Delta m_H) = \frac{L(\Delta m_H\,,\,\hat{\hat{\mu}}_{\gamma\gamma}(\Delta m_H)\,,\,\hat{\hat{\mu}}_{4\ell}(\Delta m_H)\,,\,\hat{\hat{m}}_H(\Delta m_H)\,,\,\hat{\hat{\boldsymbol{\theta}}}(\Delta m_H))}{L(\hat{\Delta m}_H, \hat{\mu}_{\gamma\gamma}, \hat{\mu}_{4\ell}, \hat{m}_H, \hat{\boldsymbol{\theta}})} . \quad (3)$$

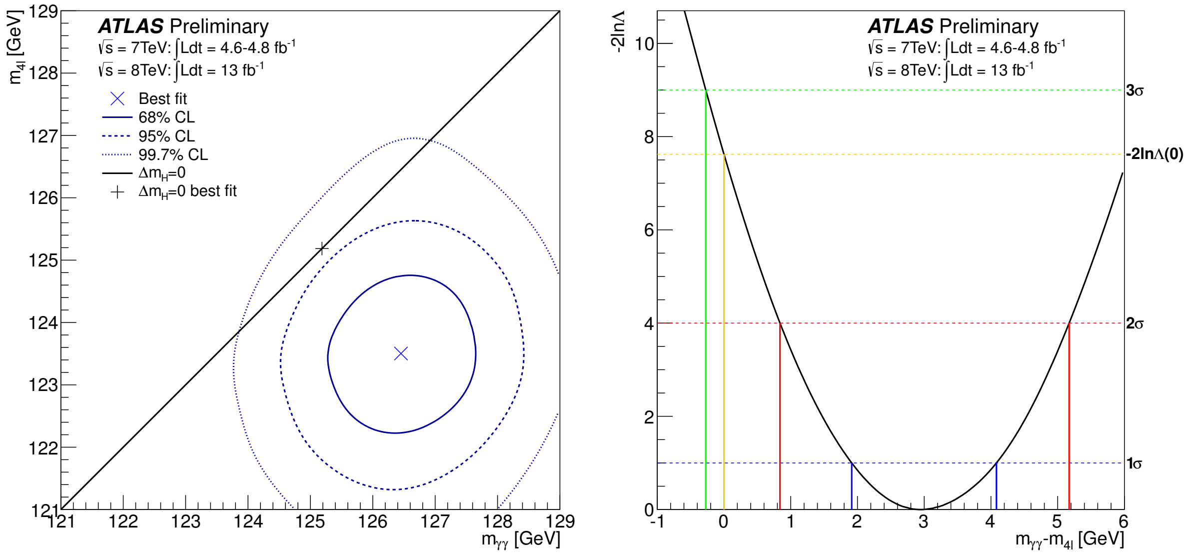

(a) (b)

Figure 2: (a) Likelihood contours as a function of $m_H^{\gamma\gamma}$ and $m_H^{4\ell}$. (b) Likelihood as a function of the mass difference, $\Delta m_H = m_H^{\gamma\gamma} - m_H^{4\ell}$, profiling over the common mass m_H. In both cases the signal strength parameters $\mu_{\gamma\gamma}$ and $\mu_{4\ell}$ are allowed to vary independently. In (a) the masses are considered as two independent parameters of interest (2-dimensional contours) while in (b) only one parameter of interest, the mass difference, is considered (1-dimensional variation of the likelihood).

This allows the hypothesis $\Delta m_H = 0$ to be tested. The signal strengths $\mu_{\gamma\gamma}$ and $\mu_{4\ell}$ are again treated as independent nuisance parameters in this approach. The likelihood is shown in Figure 2(b) as a function of the mass difference. The estimated $H\to\gamma\gamma$ and $H\to ZZ^{(*)}\to 4\ell$ mass difference is

$$\Delta\hat{m}_H = \hat{m}_H^{\gamma\gamma} - \hat{m}_H^{4\ell} = 3.0^{+1.1}_{-1.0}\ \text{GeV} = 3.0 \pm 0.8\,(\text{stat})\ ^{+0.7}_{-0.6}\,(\text{sys})\ \ \text{GeV}\ , \tag{4}$$

where the 68% CL errors are computed with the asymptotic approximation.

An important feature of the profile likelihood ratio is that asymptotically its distribution is independent of the true value of the nuisance parameters, which implies that the resulting p-values are robust. This desirable feature is not shared by other (perhaps more intuitive) quantities. Specifically, the difference between the best fit mass in the $H\to ZZ^{(*)}\to 4\ell$ and $H\to\gamma\gamma$ channels is an intuitive test statistic to use for the mass consistency, but the distribution of this mass difference is sensitive to the true and unknown values of the nuisance parameters. For this reason, the profile likelihood ratio $\Lambda(\Delta m_H = 0)$ has been adopted for testing the mass compatibility.

From the value of the likelihood evaluated at $\Delta m_H = 0$, indicated in Figure 2(b), the probability for a single Higgs boson-like particle to produce a value of the $\Lambda(\Delta m_H)$ test statistic disfavoring the $\Delta m_H = 0$ hypothesis more than observed, is found to be 0.6% (2.8σ) using the asymptotic approximation assumption, and 0.8% (2.7σ) using Monte Carlo ensemble tests[2]. The probability computed from Monte Carlo ensemble tests includes also the calibrated statistical error for $H\to ZZ^{(*)}\to 4\ell$. Further checks, assuming the SM signal strength for $H\to\gamma\gamma$ and $H\to ZZ^{(*)}\to 4\ell$, or conditioning the ensemble of pseudo-experiments to the observed signal strengths, yield similar probabilities, since μ and m_H are largely uncorrelated.

Alternatively, the significance of the mass separation is tested using rectangular pdfs for the systematic energy scale uncertainties coming from the electron energy scale extraction from the $Z\to ee$

[2]Here 2-sided probabilities are used where both cases of $m_H^{\gamma\gamma} > m_H^{4\ell}$ and $m_H^{\gamma\gamma} < m_H^{4\ell}$ are considered

sample, the imperfect knowledge of the material upstream of the electromagnetic calorimeter and the energy scale of the presampler. The rectangular pdfs give a flat *a priori* likelihood in the range of the $\pm 1\sigma$ Gaussian uncertainty intervals for these three sources of systematic uncertainties. The use of such a pdf modelling for these energy scale systematic uncertainties will lead to a coherent shift within their allowed range to values which reduce the mass difference. The overall mass difference is thus decreased by an amount corresponding to the linear sum of the individual Gaussian errors for these three sources of systematic uncertainties. With this treatment of these energy scale systematic uncertainties the probability for a single Higgs boson-like particle to produce a value of the $\Lambda(\Delta m_H)$ test statistic disfavoring the $\Delta m_H = 0$ hypothesis more than observed is found to be 2.3% (2.3σ).

6 Significance and Production Signal Strength

This section focuses on the global signal strength parameter μ for a fixed m_H. Hypothesized values of μ are tested with a statistic $\Lambda(\mu)$ based on the profile likelihood ratio [15]:

$$\Lambda(\mu; m_H) = \frac{L(\mu, \hat{\hat{\boldsymbol{\theta}}}(\mu); m_H)}{L(\hat{\mu}, \hat{\boldsymbol{\theta}}; m_H)} . \tag{5}$$

This test statistic extracts the information on the parameters of interest from the full likelihood function.

The significance of an excess in the data is quantified with the local p_0, the probability that the background can produce a fluctuation greater than or equal to the excess observed in data. The equivalent formulation in terms of number of standard deviations is referred to as the local significance.

The observed local p_0 values calculated using the asymptotic approximation and including mass scale systematic uncertainties are shown in Fig. 3 as a function of m_H. The expected p_0 corresponds to the median p_0 in the presence of a SM Higgs boson signal at that mass. The largest local significance for the combination of the 7 and 8 TeV data is found for a SM Higgs boson mass hypothesis of m_H=125.0 GeV, where it reaches 7.0σ, with an expected value in the presence of a SM Higgs boson signal at that mass of 5.9σ. As shown in previous publications, see Ref. [1], the asymptotic approximation estimate of the p_0 is less accurate in the presence of mass scale systematic uncertainties. In Ref. [1] the p_0 value obtained with the asymptotic approximation and including mass scale systematic uncertainties was found to be lower (the significance is higher by approximately 0.1 standard deviations) than the one obtained with Monte Carlo ensemble tests including the mass scale systematic uncertainties. At such a low level of probability the number of Monte Carlo ensemble tests required is prohibitively high and therefore the asymptotic approximation value is quoted in this note.

The best-fit value of μ, denoted $\hat{\mu}$, is displayed for the combination of all channels in Fig. 4 as a function of the m_H hypothesis. The bands around $\hat{\mu}$ illustrate the μ interval corresponding to $-2\ln\Lambda(\mu) < 1$ and represent an approximate $\pm 1\sigma$ variation.

The best fit values of the signal strength parameter for each channel independently and for the combination are illustrated in Fig. 5 for a mass of $m_H = 125$ GeV. The observed excess corresponds to $\hat{\mu}$ of $1.35 \pm 0.24 = 1.35 \pm 0.19\,(\text{stat}) \pm 0.15\,(\text{sys})$ for $m_H = 125$ GeV with all channels combined. This signal strength is consistent with the SM Higgs boson hypothesis $\mu = 1$. The results for the best-fit values and uncertainties are listed in Table 2. A compatibility test between the signal strengths of the five channels and the Standard Model expectation of unity gives a probability of about 13%. The dependence of the combined value of $\hat{\mu}$ on the assumed m_H has been investigated and is relatively weak: changing the mass hypothesis between 123.5 and 126.5 GeV changes the value of $\hat{\mu}$ by about 10%.

In order to test which values of the strength and mass of a signal hypothesis are simultaneously consistent with the data, the profile likelihood ratio $\Lambda(\mu, m_H)$ is used. Asymptotically, the test statistic $-2\ln\Lambda(\mu, m_H)$ is distributed as a χ^2 distribution with two degrees of freedom. The resulting 68% and

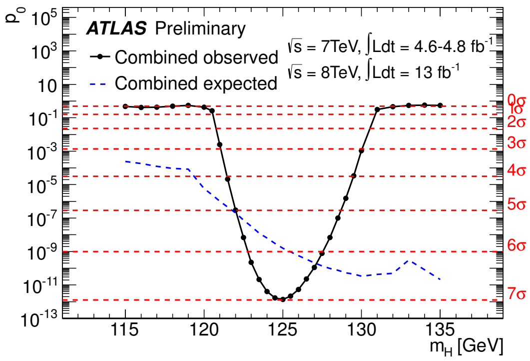

Figure 3: The local probability p_0 for a background-only experiment to be more signal-like than the observation as a function of m_H. The dashed curve shows the median expected local p_0 under the hypothesis of a production of a Standard Model Higgs boson with that mass. The horizontal dashed lines indicate the p-values corresponding to significances of 0σ to 7σ. Mass scale systematic uncertainties are included.

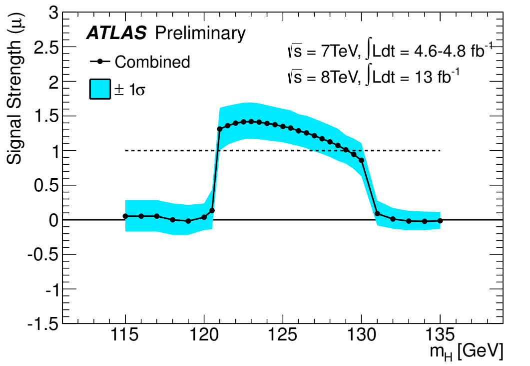

Figure 4: The combined best-fit signal strength $\hat{\mu}$ as a function of m_H. The interval around $\hat{\mu}$ corresponds to a variation of $-2\ln\Lambda(\mu) < 1$. Mass scale systematic uncertainties are included, which leads to a broad peak as described in Ref. [5].

Table 2: Summary of the best-fit values and uncertainties for the signal strength μ for the individual channels at a Higgs boson mass of 125 GeV.

Higgs Boson Decay	μ (m_H=125 GeV)
$VH \to Vbb$	-0.4 ± 1.0
$H \to \tau\tau$	0.8 ± 0.7
$H \to WW^{(*)}$	1.5 ± 0.6
$H \to \gamma\gamma$	1.8 ± 0.4
$H \to ZZ^{(*)}$	1.0 ± 0.4
Combined	1.35 ± 0.24

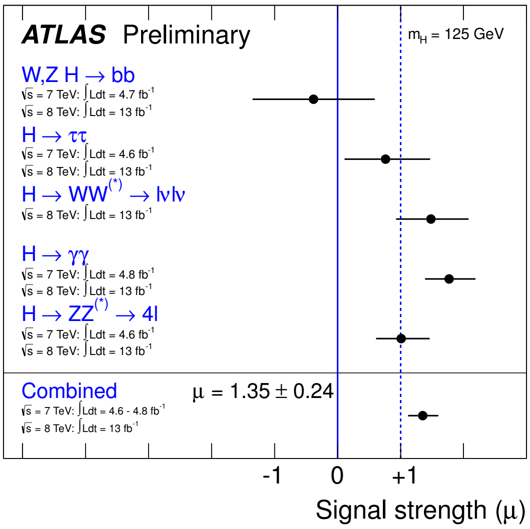

Figure 5: Measurements of the signal strength parameter μ for m_H =125 GeV for the individual channels and for their combination.

95% CL contours for the $H\to\gamma\gamma$ and $H\to ZZ^{(*)}\to 4\ell$ channels are shown in Fig. 6. In this case, neither the m_H value that minimizes p_0 nor the one that maximizes $\hat{\mu}$ are unbiased estimates of the SM Higgs boson mass m_H as they are computed using a fixed m_H hypothesis. The maximum likelihood estimate presented in Section 5 is the appropriate estimator for the mass.

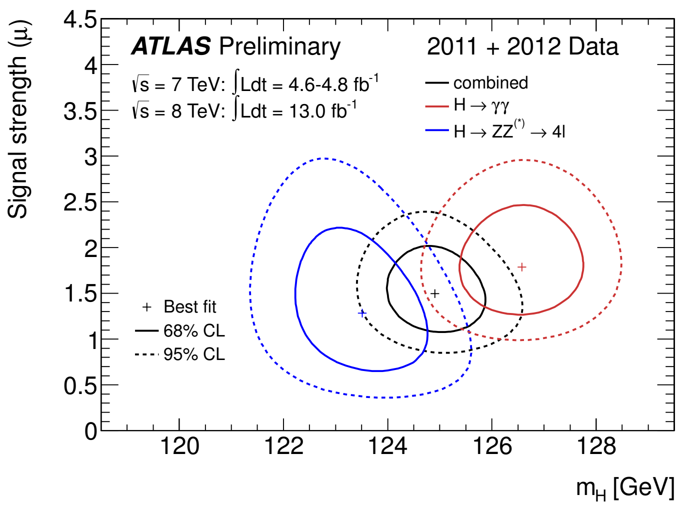

Figure 6: Confidence intervals in the (μ, m_H) plane for the $H\to ZZ^{(*)}\to 4\ell$ and $H\to\gamma\gamma$ channels and their combination, including all systematic uncertainties. The markers indicate the maximum likelihood estimates $(\hat{\mu}, \hat{m}_H)$ in the corresponding channels.

7 Conclusion

An update is presented of the properties of the newly discovered Higgs-like boson using the data set corresponding to up to 4.8 fb^{-1} of pp collision data at $\sqrt{s}$ = 7 TeV and 13 fb^{-1} at $\sqrt{s}$ = 8 TeV.

The mass measurement, based on fits to the spectra of the high mass resolution channels $H \rightarrow \gamma\gamma$ and $H \rightarrow ZZ^{(*)} \rightarrow 4\ell$, is $m_H = 125.2 \pm 0.3\,(\text{stat}) \ \pm 0.6\,(\text{sys})$ GeV. The difference of the mass measurements between the two channels is $3.0 \pm 0.8\,(\text{stat})\ ^{+0.7}_{-0.6}\,(\text{sys})$ GeV, corresponding to about 2.7 standard deviations, using Gaussian pdfs for systematic uncertainties. A more conservative treatment of the systematic uncertainty related to the mass scale, using rectangular pdfs for parts of the error, reduces the difference to the level of 2.3 standard deviations. The measurement of the signal strengths for the final states $H \rightarrow \gamma\gamma$, $H \rightarrow ZZ^{(*)} \rightarrow 4\ell$, $H \rightarrow WW^{(*)} \rightarrow \ell\nu\ell\nu$, $H \rightarrow \tau^+\tau^-$ and $H \rightarrow b\bar{b}$ have been combined giving an average value of $1.35 \pm 0.19\,(\text{stat}) \pm 0.15\,(\text{sys})$ computed at the mass of 125 GeV. A compatibility test between the observed signal strengths of the five channels and the Standard Model expectation of unity gives a probability of about 13%. The measured properties of the new boson are consistent with the expectations of the Standard Model Higgs boson.

References

[1] ATLAS Collaboration, *Observation of a new particle in the search for the Standard Model Higgs boson with the ATLAS detector at the LHC*, Phys. Lett. **B 716** (2012) 1–29, arXiv:1207.7214 [hep-ex].

[2] CMS Collaboration, *Observation of a new boson at a mass of 125 GeV with the CMS experiment at the LHC*, Phys. Lett. **B 716** (2012) 30–61, arXiv:1207.7235 [hep-ex].

[3] ATLAS Collaboration, *Coupling properties of the new Higgs-like boson observed with the ATLAS detector at the LHC*, ATLAS-CONF-2012-127 (2012).

[4] ATLAS Collaboration, *Updated ATLAS results on the signal strength of the Higgs-like boson for decays into WW and heavy fermion final states*, ATLAS-CONF-2012-162 (2012).

[5] ATLAS Collaboration, *Observation and study of the Higgs boson candidate in the two photon decay channel with the ATLAS detector at the LHC*, ATLAS-CONF-2012-168 (2012).

[6] ATLAS Collaboration, *Updated results and measurements of properties of the new Higgs-like particle in the four lepton decay channel with the ATLAS detector*, ATLAS-CONF-2012-169 (2012).

[7] ATLAS Collaboration, *Search for the Standard Model Higgs boson in $H \to \tau\tau$ decays in proton-proton collisions with the ATLAS detector*, ATLAS-CONF-2012-160 (2012).

[8] ATLAS Collaboration, *Search for the Standard Model Higgs boson in produced in association with a vector boson and decaying to bottom quarks with the ATLAS detector*, ATLAS-CONF-2012-161 (2012).

[9] ATLAS Collaboration, *Update of the $H \to WW^{(*)} \to \ell\nu\ell\nu$ Analysis with 13 fb^{-1} of $\sqrt{s} = 8$ TeV Data Collected with the ATLAS Detector*, ATLAS-CONF-2012-158 (2012).

[10] ATLAS Collaboration, *Combined search for the Standard Model Higgs boson in pp collisions at $\sqrt{s}$=7 TeV with the ATLAS detector*, Phys. Rev. **D86** (2012) 032003, arXiv:1207.0319 [hep-ex].

[11] ATLAS and CMS Collaborations, *Procedure for the LHC Higgs boson search combination in Summer 2011*, ATL-PHYS-PUB-2011-011, CERN-CMS-NOTE-2011-005 (2011). http://cdsweb.cern.ch/record/1375842.

[12] L. Moneta, K. Belasco, K. S. Cranmer, S. Kreiss, A. Lazzaro, et al., *The RooStats Project*, PoS **ACAT2010** (2010) 057, arXiv:1009.1003 [physics.data-an].

[13] K. Cranmer, G. Lewis, L. Moneta, A. Shibata, and W. Verkerke, *HistFactory: A tool for creating statistical models for use with RooFit and RooStats*, CERN-OPEN-2012-016 (2012). http://cdsweb.cern.ch/record/1456844.

[14] W. Verkerke and D. Kirkby, *The RooFit toolkit for data modelling*, Tech. Rep. physics/0306116, SLAC, Stanford, CA, Jun, 2003. arXiv:physics/0306116v1 [physics.data-an].

[15] G. Cowan, K. Cranmer, E. Gross, and O. Vitells, *Asymptotic formulae for likelihood-based tests of new physics*, Eur. Phys. J. **C71** (2011) 1554.

[16] ATLAS Collaboration, *Combined search for the Standard Model Higgs boson in pp collisions at $\sqrt{s}$ = 7 TeV with the ATLAS detector*, submitted to Phys. Rev. D (2012), arXiv:1207.0319 [hep-ex].

Appendix

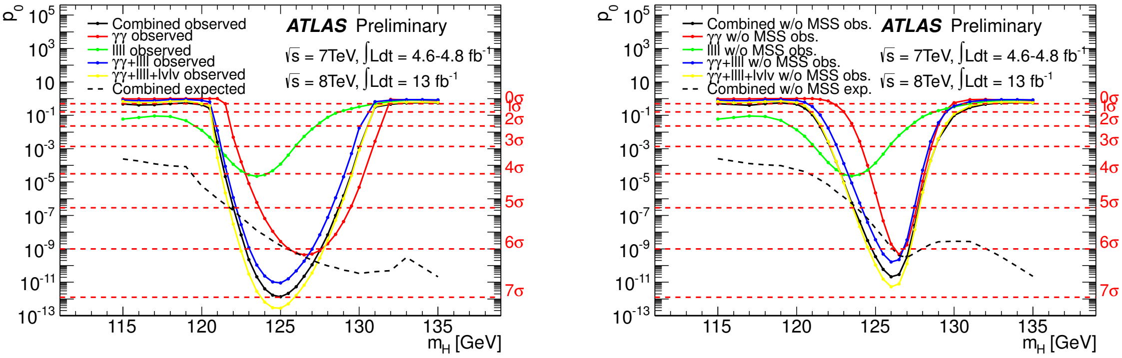

(a) (b)

Figure 7: The local probability p_0 for a background-only experiment to be more signal-like than the observation as a function of m_H for various progressive cases of combinations: $H\to\gamma\gamma$ (red line); $H\to ZZ^{(*)}\to 4\ell$ (green line); combination of $H\to\gamma\gamma$ and $H\to ZZ^{(*)}\to 4\ell$ (blue line); combination of $H\to\gamma\gamma$, $H\to ZZ^{(*)}\to 4\ell$ and $H\to WW^{(*)}\to \ell\nu\ell\nu$ (magenta line) and the combination of all channels, including $H\to b\bar{b}$ and $H\to\tau^+\tau^-$ (black line). The dashed black curve shows the median expected local p_0 under the hypothesis of a Standard Model Higgs boson production signal at that mass for the combination of all channels. The horizontal dashed lines indicate the p-values corresponding to significances of 0σ to 7σ. For (a) mass scale systematic uncertainties are included with the asymptotic approximation, while (b) is without the mass scale systematic uncertainties, which reduces the compatibility of the different channels and hence reduces the overall significance.

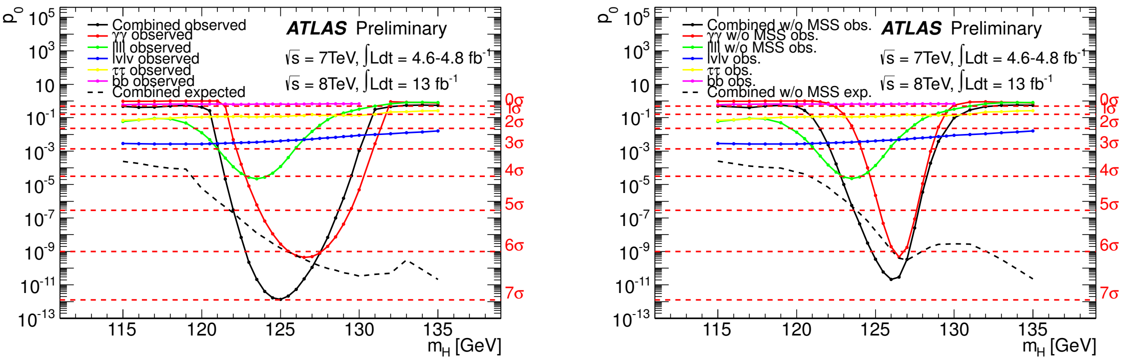

(a) (b)

Figure 8: The local probability p_0 for a background-only experiment to be more signal-like than the observation as a function of m_H for various individual channels: $H\to\gamma\gamma$ (red line); $H\to ZZ^{(*)}\to 4\ell$ (green line); $H\to WW^{(*)}\to \ell\nu\ell\nu$ (blue line); $H\to\tau^+\tau^-$ (yellow line); $H\to b\bar{b}$ (magenta line) and the combination of all channels (black line). For (a) mass scale systematic uncertainties are included with the asymptotic approximation, while (b) is without the mass scale systematic uncertainties, which reduces the compatibility of the different channels and hence reduces the overall significance.

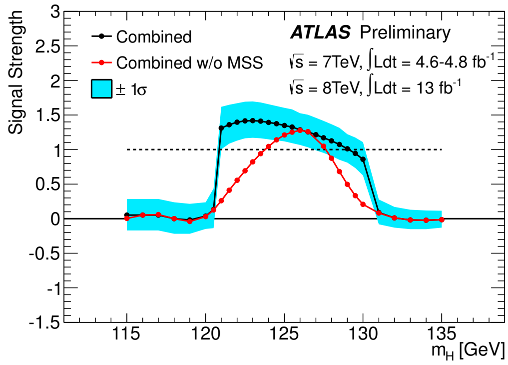

(a)

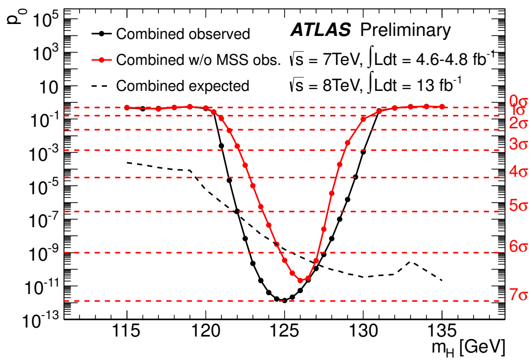

(b)

Figure 9: (a) The combined best-fit signal strength $\hat{\mu}$ as a function of m_H and (b) the local probability p_0 for a background-only experiment to be more signal-like than the observation as a function of m_H shown once with (black line) and once without (red line) mass scale systematic uncertainties. As shown in previous publications, see Ref. [1], the asymptotic approximation estimate of the p_0 is less accurate in the presence of mass scale systematic uncertainties. In Ref. [1] the p_0 value obtained with the asymptotic approximation and including mass scale systematic uncertainties was found to be lower (the significance is higher by approximately 0.1 standard deviations) than the one obtained with Monte Carlo ensemble tests including the mass scale systematic uncertainties.

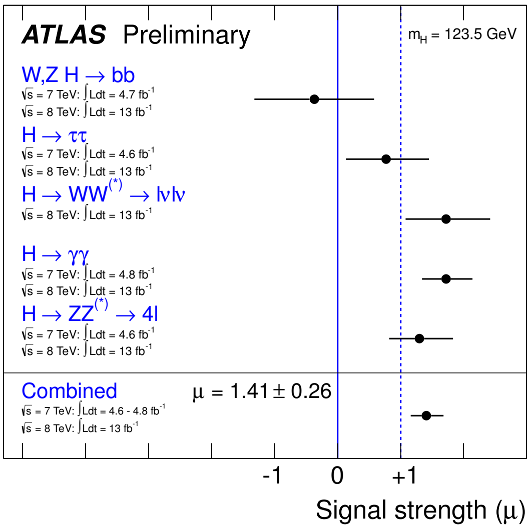

(a)

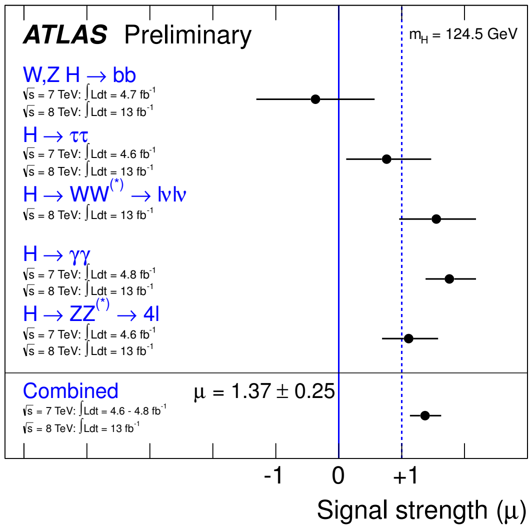

(b)

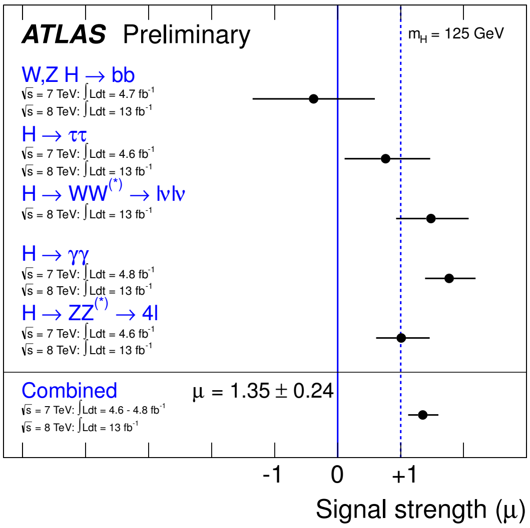

(c)

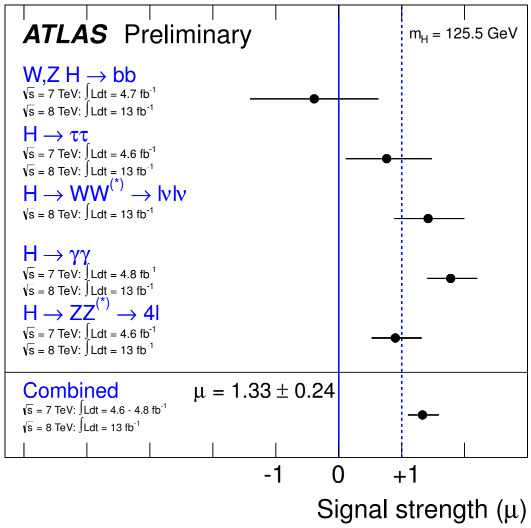

(d)

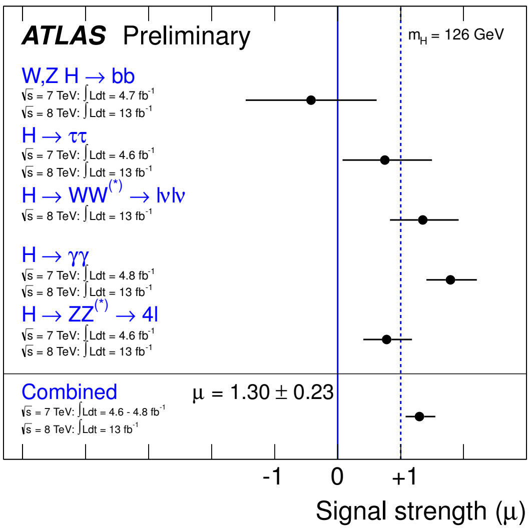

(e)

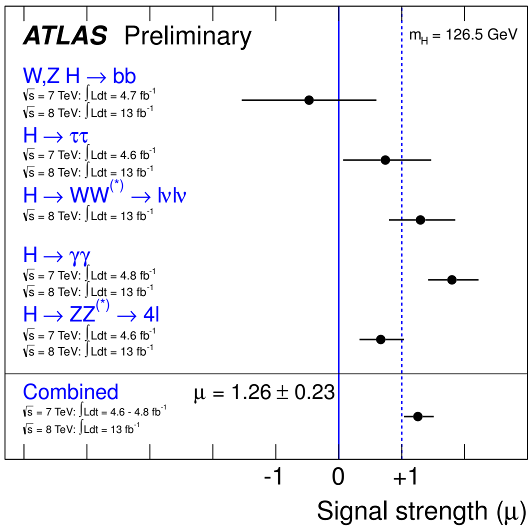

(f)

Figure 10: Measurements of the signal strength parameter μ for m_H between 123.5 GeV and 126.5 GeV for the individual channels and their combination.

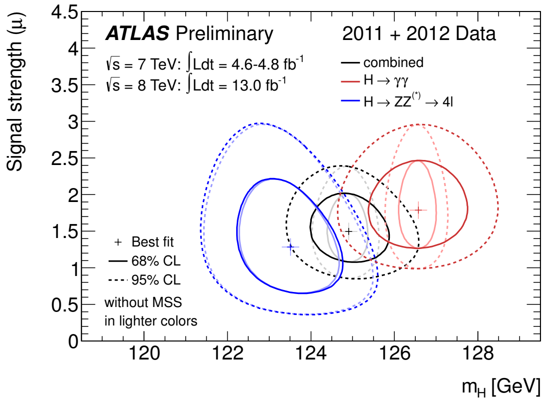

Figure 11: Confidence intervals in the (μ, m_H) plane for the $H\rightarrow ZZ^{(*)}\rightarrow 4\ell$ and $H\rightarrow\gamma\gamma$ channels and their combination, including all systematic uncertainties (thick lines) and without the mass scale systematic (MSS) uncertainties (thin lines in lighter colors). The markers indicate the maximum likelihood estimates $(\hat{\mu}, \hat{m}_H)$ in the corresponding channels.